SAND--98-8481C
CONF-980804--

# Statistics of Flame Displacement Speeds from Computations of 2-D Unsteady Methane-Air Flames

RECEIVED
MAR 2 7 1998
OSTI

N. Peters[1] and P. Terhoeven

Institut für Technische Mechanik, RWTH Aachen, Germany

Phone (49)-241-804609

FAX (49)-241-8888223

e-mail: n.peters@itm.rwth-aachen.de

Jacqueline H. Chen and Tarek Echekki

Combustion Research Facility, Sandia National Laboratories, Livermore, CA 94551 0969, USA

A manuscript for the 27th Symposium on Combustion

Colloquium topic: Turbulent Premixed and Partially Premixed Combustion

Key words: displacement speeds, thin reaction zones

Total word count: 2400 text, 2400 in figures, 175 in nomenclature

and 441 in equations = 5416 words total

December 8, 1997

[1]corresponding author

## DISCLAIMER

Results of two-dimensional numerical computations of turbulent methane flames using detailed and reduced chemistry are analyzed in the context of a new theory for premixed turbulent combustion for high turbulence intensity. This theory defines the thin reaction zones regime, where the Kolmogorov scale is smaller than the preheat zone thickness, but larger than the reaction zone thickness. The two numerical computations considered in this paper fall clearly within this regime. A lean and a stoichiometric flame are considered. The former is characterized by a large ratio of the turbulence intensity to the laminar burning velocity and the latter by a smaller value of that ratio.

The displacement speed of the reaction zone relative to the flow is defined as the displacement speed of the iso-scalar line at a fuel mass fraction corresponding to 10% of the upstream value. The three different mechanisms that are contributing to the displacement of the reaction zone, namely normal and tangential diffusion and reaction, are analyzed and their probability density functions are evaluated. Although these contributions fluctuate considerably, the mean value of the overall displacement speed is found to be only around 40% larger than the burning velocity of a plane premixed flame at the same equivalence ratio. Furthermore, the contribution of tangential diffusion, which can be expressed as a curvature term, cancels as far as the mean overall displacement speed is concerned, while the contributions of normal diffusion and reaction are large but have opposite signs. These contributions depend implicitly on curvature. This dependence is small for the lean flame, but considerable for the stoichiometric flame where it leads to an enhanced diffusivity. This diffusivity is compared to the Markstein diffusivity that describes the equivalent curvature effect in the corrugated flamelet regime.

## NOMENCLATURE

| | |
|---|---|
| $D$ | mass diffusion coefficient of $CH_4$ |
| $G$ | distance function |
| $\ell$ | integral length scale |
| $\ell_F$ | laminar flame thickness |
| $\ell_\delta$ | reaction zone thickness |
| $\vec{n}$ | normal vector |
| $s$ | arclength |
| $s_d$ | displacement speed |
| $s_L$ | laminar burning velocity |
| $V_n$, $V_r$ | displacement speed contributions due to normal diffusion and reaction, respectively |
| $v'$ | turbulence intensity |
| $\vec{v}$ | flow velocity vector |
| $x$, $y$ | coordinates in the 2D simulation |
| $Y$ | mass fraction |

Greek Symbols

| | |
|---|---|
| $\delta$ | $= \ell_\delta / \ell_F$ non-dimensional reaction zone thickness |
| $\phi$ | fuel-to-air equivalence ratio |
| $\kappa$ | curvature of the reaction zone, defined as positive if the front is convex towards the unburnt mixture |
| $\rho$ | density |
| $\eta$ | Kolmogorov length scale |
| $\dot{\omega}$ | reaction rate |

Indices

| | |
|---|---|
| 0 | at the thin reaction zone |
| $u$ | in the unburnt |
| $CH_4$ | methane |

# 1 Introduction

There have been different views about the physical mechanisms that are important in the regime of turbulent premixed combustion where the Kolmogorov scale $\eta$ is smaller than the flame thickness $\ell_F$. Borghi [1] has called it the regime of "thickened-wrinkled flame with possible extinction", Peters [2] calls it the "distributed reaction zones" regime and Poinsot et al. [3] consider it to be part of the flamelet regime. Poinsot et al. have performed direct 2D numerical simulations of vortices interacting with flame structures and find that these "are more resistant to quenching" and that therefore the flamelet region extends by "more than an order of magnitude" into the regime where the Kolmogorov scale is smaller than the flame thickness.

Recently, Peters [4] defined a regime called the "thin reaction zones regime" by

$$\ell_\delta < \eta < \ell_F \tag{1}$$

where Kolmogorov eddies can penetrate into the preheat zone of size $\ell_F$ but not into the reaction zone of size $\ell_\delta$. The thickness of the thin reaction zone is typically one tenth of that of the preheat zone, but the ratio $\delta = \ell_\delta/\ell_F$ may vary with pressure and the temperature of the unburnt gas [5]. The thin reaction zones regime is shown in a diagram, Fig. 1, where the velocity ratio $v'/s_L$ is plotted as a function of the length scale ratio. The conditions that will be analyzed here correspond to methane-air flames: a lean flame [6] denoted by LF and a stoichiometric flame [7] denoted by SF.

For the lean flame a detailed mechanism based on $C_1$ chemistry [8] and for the stoichiometric flame a four-step reduced mechanism [9] has been employed. For computational efficiency a preheat temperature of 800K was assumed. The turbulent velocity field is super-imposed on the evolving scalar fields and decays with time. It is prescribed by an initial two-dimensional turbulent kinetic energy spectrum function. Note that the points indicated in Fig. 1 correspond to the initial condition, while the evaluations are performed after 2.11 turnover times for the lean flame and one turnover time for the stoichiometric flames. At those times the turbulence intensity has decayed by 5% for both flames.

## 2 Formulation

Since small eddies are able to penetrate into the preheat zone of the flame structure in the thin reaction zones regime, the scalar field in front of the reaction zone is perturbed by turbulence and a quasi-steady state flame structure does not exist. Molecular transport between the thin reaction zone and the upstream temperature and concentration fields is an unsteady process and the notion of a laminar burning velocity has no physical meaning. We may, however, define a displacement speed of the thin reaction zone relative to the flow by considering a scalar iso-surface in the vicinity of the reaction zone. Since the fuel is entirely consumed in the inner layer of methane flames and it decreases monotonically between the unburnt conditions upstream and the inner layer, an iso-contour of 10% of the fuel mass fraction $Y_{CH_4}$ was considered to be the most representative choice. Several levels of $Y_{CH_4}$ were examined and it was found that within the range between 5% and 30% of the upstream value the results did not depend very much on that choice.

Consider the balance equation of the fuel

$$\rho\left(\frac{\partial Y_{CH_4}}{\partial t} + \vec{v}\cdot\nabla Y_{CH_4}\right) = \nabla\cdot(\rho D \nabla Y_{CH_4}) + \dot{\omega}_{CH_4} \qquad (2)$$

where $D$ is its diffusion coefficient and $\dot{\omega}_{CH_4}$ its chemical source term. The iso-scalar surface

$Y_{\mathrm{CH_4}}(\vec{x}, t) = Y_0$, where $Y_0$ denotes 0.1 $Y_{\mathrm{CH_4},u}$, must satisfy the condition

$$\frac{\partial Y_{\mathrm{CH_4}}}{\partial t} + \nabla Y_{\mathrm{CH_4}} \cdot \left.\frac{d\vec{x}}{dt}\right|_0 = 0\,. \qquad (3)$$

Replacing $\partial Y_{\mathrm{CH_4}}/\partial t$ from Eq. (2) this leads to

$$\left.\frac{d\vec{x}}{dt}\right|_0 = \vec{v}_0 - \left[\frac{\nabla\cdot(\rho D \nabla Y_{\mathrm{CH_4}}) + \dot{\omega}_{\mathrm{CH_4}}}{\rho|\nabla Y_{\mathrm{CH_4}}|}\right]_0 \vec{n} = \vec{v}_0 + s_d \vec{n}\,. \qquad (4)$$

Here the term in square brackets is the displacement speed $s_d$ of the thin reaction zone. For diffusive scalars with $\dot{\omega} = 0$ Eq. (4) was first derived in [10]. The normal vector on the iso-mass-fraction surface points towards the unburnt mixture and is defined as

$$\vec{n} = \frac{\nabla Y_{\mathrm{CH_4}}}{|\nabla Y_{\mathrm{CH_4}}|}\,. \qquad (5)$$

We want to use the analogy between the laminar burning velocity of a quasi-steady flame structure and the displacement speed for the thin reaction zone and derive a $G$-equation for the location of the thin reaction zone in analogy to the classical $G$-equation [11] where the flame location is defined by the iso-surface $G(\vec{x}, t) = G_0$. Then the normal vector defined by Eq. (5) is also equal to

$$\vec{n} = -\frac{\nabla G}{|\nabla G|} \qquad (6)$$

and also points towards the unburnt mixture. Using the evolution equation for the iso-scalar surface $G(x, t) = G_0$

$$\frac{\partial G}{\partial t} + \nabla G \cdot \frac{d\vec{x}}{dt}\Big|_{G=G_0} = 0 \qquad (7)$$

together with Eq. (4) leads to

$$\frac{\partial G}{\partial t} + \vec{v}_0 \cdot \nabla G = -\left[\frac{\nabla\cdot(\rho D \nabla Y_{\mathrm{CH_4}}) + \dot{\omega}_{\mathrm{CH_4}}}{\rho|\nabla Y_{\mathrm{CH_4}}|}\right]_0 |\nabla G|\,. \qquad (8)$$

Echekki and Chen [12] show that the diffusive term appearing on the r.h.s of Eq. (8) may be split into one term accounting for curvature and another for diffusion normal to the iso-surface

$$\nabla \cdot (\rho D \nabla Y_{CH_4}) = \rho D |\nabla Y_{CH_4}| \kappa + \vec{n} \cdot \nabla(\rho D \vec{n} \cdot \nabla Y_{CH_4}) \tag{9}$$

where the definition Eq. (5) has been used. When Eq. (9) is introduced into Eq. (8) it can be written as

$$\frac{\partial G}{\partial t} + \vec{v}_0 \cdot \nabla G = -D\,\kappa |\nabla G| + (V_n + V_r)|\nabla G| \,. \tag{10}$$

Here the curvature $\kappa$ may be expressed by Eq. (11) in terms of the $G$-field as

$$\kappa = \nabla \cdot \vec{n} = \nabla \cdot \left( -\frac{\nabla G}{|\nabla G|} \right) = -\frac{\nabla^2 G - \vec{n} \cdot \nabla(\vec{n} \cdot \nabla G)}{|\nabla G|} \,. \tag{11}$$

The quantities $V_n$ and $V_r$ are contributions due to normal diffusion and reaction to the displacement speed of the thin reaction zone and are defined as in [13] as

$$V_n = -\frac{\vec{n} \cdot \nabla(\rho D \vec{n} \cdot \nabla Y_{CH_4})}{\rho |\nabla Y_{CH_4}|} \tag{12}$$

$$V_r = -\frac{\dot{\omega}_{CH_4}}{\rho |\nabla Y_{CH_4}|} \,. \tag{13}$$

In a steady, unstretched planar laminar flame the sum of $V_n$ and $V_r$ would be equal to the burning velocity $s_L$. Here, however, the unsteady mixing and diffusion of all the chemical species and the temperature in the regions ahead and behind the thin reaction zones will influence the local displacement speed. Therefore the sum of $V_n$ and $V_r$ cannot be prescribed, but is a fluctuating quantity, that couples the $G$-equation to the solution of the balance equations of the reactive scalars.

Finally, in view of Eqs. (4), (9), (12) and (13) it should be noted that the three contributions to the displacement speed add up as

$$s_d = -D\kappa + V_n + V_r \tag{14}$$

where $-D\kappa$ is the contribution due to curvature.

In Fig. 2 iso-mass-fraction lines and iso-scalar lines of $G$ are plotted for a flame contour taken from the lean flame [6]. The flame propagates from right to left. The coordinates $x$ and $y$ were normalized by the flame thickness for a plane laminar lean methane flame at $\phi = 0.7$. The dark black line in Figs. 2a and 2b denote the location of the thin reaction zone at $Y_{CH_4} = 0.1\,Y_{CH_4,u}$. In Fig. 2a, in addition, iso-mass-fraction contours of $Y_{CH_4} = 0.5\,Y_{CH_4,u}$ and of $0.9\,Y_{CH_4,u}$ are shown. Contours of the distance function $G = -0.5$ and $G = -1.0$ are shown in Fig. 2b. They correspond to lines with a distance of one half and one flame thickness ahead of the reaction zone. The comparison between the two plots shows that except for regions where the reaction zone is strongly curved, the $Y_{CH_4} = 0.5\,Y_{CH_4,u}$ line and the $G = -0.5$ line do not differ very much from each other. For the stoichiometric flame the iso-mass fraction line at $Y_{CH_4} = 0.1\,Y_{CH_4,u}$ is shown in Fig. 3. The coordinates are normalized by the corresponding flame thickness.

## 3 Statistical Evaluation

We have evaluated the different contributions to the displacement speed at the 10% fuel mass-fraction iso-line and normalized it by the displacement speed $s_{L,0}$ of the reaction zone in a one-dimensional normal flame

$$s_{L,0} = \frac{\rho_u s_{L,u}}{\rho_0} \tag{15}$$

where $\rho_u$ and $s_{L,u}$ are the unburnt values for a plane laminar flame at the corresponding equivalence ratio. Figs. 4a and 4b show for both flames the normalized displacement speed $s_d$ as well as the contributions $V_r$, $V_n$ and $-D\kappa$ that appear in Eq. (14). They are plotted over the arclength normalized by the flame thickness. The arclength is counted from lower entry to the upper exit in Figs. 2a and 3, respectively. The maximum displacement speed of the lean flame

(Fig. 4a) occurs at $s/\ell_F = 52$ which corresponds to the strongly curved region far on the right in Fig. 2a. There are several maxima in the stoichiometric flame (Fig. 4b). The oscillations of $s_d$ are quite substantial, with part of the iso-line at values below $s_d/s_{L,0} = 1$, but strong positive excursions. The positive excursions are mainly due to an addition of contributions from reaction and curvature, while the contribution of normal diffusion seems to be negatively correlated with that of the curvature. All contributions to the displacement speed fluctuate very strongly. Since $CH_4$ is always consumed at the location $Y_{CH_4} = 0.1\,Y_{CH_4,u}$ the contribution due to reaction is always positive. Its magnitude at this location is still very large because the flames are preheated to 800K. It is interesting to note that the contribution due to normal diffusion is always negative and that due to curvature fluctuates around zero. Note that the mean curvature is zero due to cyclic boundary conditions imposed on the lower and upper side in Figs. 2a and 3.

The probability density functions (pdfs) of the different contributions for both flames are shown in Figs. 5 and 6. The pdfs of the contributions due to normal diffusion, reaction and curvature are shown in Fig. 5 for both flames. Again it is seen that the pdf of $V_n$ lies at negative values with a mean value at -4.71 for the lean flame and at -1.74 for the stoichiometric flame. The pdf of $V_r$ is at positive values with a mean at 6.06 for the lean flame and at 2.93 for the stoichiometric flame. The pdf of $-D\kappa$ is nearly symmetric around the origin for both flames. When the pdfs of the sum of $V_r + V_n$ are plotted in Fig. 6 and compared to the pdfs of $s_d$, the mean values of $s_d$ and of the sum of $V_r + V_n$ are both equal to 1.35 for the lean flame and 1.45 for the stoichiometric flame. It is seen that, within the accuracy of the limited amount of data, the two pdfs nearly coincide for both flames. The sum of $V_r$ and $V_n$ would be equal to $s_d$ in a normal flame, but it can be seen from Fig. 4 that $V_r$ and $V_n$ do not locally add up to $s_d$ along the arclength. Therefore it is interesting to note that their statistical distribution is nearly the same.

In the theory developed in [4] the importance of the curvature term for turbulent flame propagation in the thin reaction zones regime was emphasized. Highly curved regions are due to the interaction of the reaction zone with very small eddies. Thereby the surface area of the reaction zone is strongly increased. In Eq. (10) the displacement speed due to curvature has been separated from those due to normal diffusion and reaction. It is interesting to analyze, however, whether there are interdependencies between these terms, in particular whether $V_r$ and $V_n$ implicitly also depend on curvature. Fig. 7 presents scatter plots of the different contributions to $s_d$ as a function of the curvature normalized with $\ell_F$ for both flames. It is clear that the displacement speed due to the curvature $-D\,\kappa$ must correspond to straight lines through the origin with a negative slope in these plots. In Fig. 7a and 7b the curvature has been normalized by the thermal flame thickness. Since the slope of the normalized contribution due to curvature is minus one in Fig. 7a but -0.24 in Fig. 7b, the flame thickness is related to the diffusivity as $\ell_F = D/s_{L,0}$ for the lean flame, but as $\ell_F = 4.166\,D/s_{L,0}$ for the stoichiometric flame.

The negative correlation between the displacement speed due to normal diffusion and that due to curvature that had been noted in the discussion of Fig. 4 is clearly seen for positive values of $\kappa$ (negative curvature displacement speeds). There does not seem to be much correlation between $V_r$ and $\kappa$ for positive values of $\kappa$, but for negative values of $\kappa$ they seem to be correlated. This correlation is attributed to the enhanced differential diffusion of light radical species, which, through chemical nonlinearity enhances $V_r$ indirectly [7].

Since the majority of points fall on top of each other in these scatter plots they tend to be misleading as far as mean tendencies are concerned. If a linear fit through the data points in Fig. 6 is performed it turns out that for the lean flame the displacement speeds are correlated as

$$
\begin{aligned}
V_n/s_{L,0} &= -4.70 + 0.42\,\kappa\,\ell_F \\
V_r/s_{L,0} &= 6.08 - 0.28\,\kappa\,\ell_F\,.
\end{aligned}
\tag{16}
$$

Therefore the sum

$$
(V_r + V_n)/s_{L,0} = 1.37 - 0.14\,\kappa\,\ell_F \tag{17}
$$

is nearly independent of curvature. On the contrary, for the stoichiometric flame the correlations are

$$
\begin{aligned}
V_n/s_{L,0} &= -1.47 + 0.09\,\kappa\,\ell_F \\
V_r/s_{L,0} &= 2.91 - 0.55\,\kappa\,\ell_F
\end{aligned}
\tag{18}
$$

with the sum

$$
(V_r + V_n)/s_{L,0} = 1.44 - 0.44\,\kappa\,\ell_F\,. \tag{19}
$$

This seems to justify the decomposition of the displacement speed into a curvature term and a term containing the sum of $V_n + V_r$ in Eq. (10) for the lean flame, but not for the stoichiometric flame. If one introduces Eq. 19 into Eq. 14 one obtains

$$
s_d = -2.83\,D\,\kappa + 1.44\,s_{L,0} \tag{20}
$$

showing an effective diffusivity that is 2.83 times the mass diffusivity. The reason for this enhanced diffusivity may lie in the fact that the stoichiometric flame is close to the corrugated flamelet regime (cf. Fig. 2). In that regime the Markstein diffusivity replaces the mass diffusivity. Since the Markstein diffusivity is two to three times larger than the mass diffusivity in stoichiometric methane flames [14], one may argue that the increased effective diffusivity for this flame is due to Markstein effects.

## Summary

The statistical evaluation of the different contributions to the displacement speed from two 2-D simulations shows that those due to normal diffusion and reaction are responsible for flame displacement in the mean which is approximately 40% larger than in the corresponding laminar flame. Although they fluctuate strongly when plotted over arclength, their sum has nearly the same probability density function as the displacement speed. There is still a correlation between curvature and the displacement speeds due to reaction and normal diffusion, at least for the stoichiometric flame.

## Acknowledgements

This work has been supported by the Deutsche Forschungsgemeinschaft and the U.S. Department of Energy's Office of Basic Energy Sciences, Chemical Science Division.

## References

[1] Borghi, R. W., In *Recent Advances in the Aerospace Science* (Ed. C.Casci), pp 117 138, Plenum Press, 1985.

[2] Peters, N., In *Twenty-First Symposium (International) on Combustion*, The Combustion Institute, Pittsburgh, PA, 1986, pp 1231–1250.

[3] Poinsot, T., Veynante, D., and Candel, S., In *Twenty-Third Symposium (International) on Combustion*, The Combustion Institute, PA, 1990, pp 613–619.

[4] Peters, N., *The Turbulent Burning Velocity for Large Scale and Small Scale Turbulence*, submitted to the J. of Fluid Mechanics, 1997.

[5] Peters, N., In *Numerical Approaches to Combustion Modelling* (S. Oran and J. P. Boris, Eds.), Progr. Astronautics and Aeronautics 135:155–182, 1991 .

[6] Chen, J. H. and Echekki, T., *Pocket Formation in Turbulent Lean Premixed Methane-Air Flames*, submitted to *Combust.Flame* (1997).

[7] Echekki, T. and Chen, J. H., *Combust.Flame* 106:184–202 (1996).

[8] Warnatz, J., Maas, U. and Dibble, R., Combustion: *Physical and Chemical Foundations, Modelling, Pollutant Formation*, Springer-Verlag, Heidelberg, Germany, 1996.

[9] Peters, N., and Williams, F. A., *Combust.Flame* 68:185–207 (1987).

[10] Gibson, C. H., Phys.Fluids 11:2305–2315 (1968).

[11] Williams, F. A., In *The Mathematics of Combustion* (J. D. Buckmaster, Ed.) Society for Industrial and Applied Mathematics, Philadelphia, 1985, pp 97–131.

[12] Echekki, T. and Chen, J. H., *Analysis and Computation of Different Contributions to Flame Propagation in Turbulent Premixed Methane-Air Flames*, submitted to *Combust.Flame* 1997.

[13] Gran, I. R., Echekki, T., and Chen, J. H., In *Twenty-Sixth Symposium (International) on Combustion*, The Combustion Institute, Pittsburgh, PA, 1996, pp 323–329.

[14] Müller, U. C., Bollig, M., Peters, N., *Combust.Flame* 108:349–356 (1997).

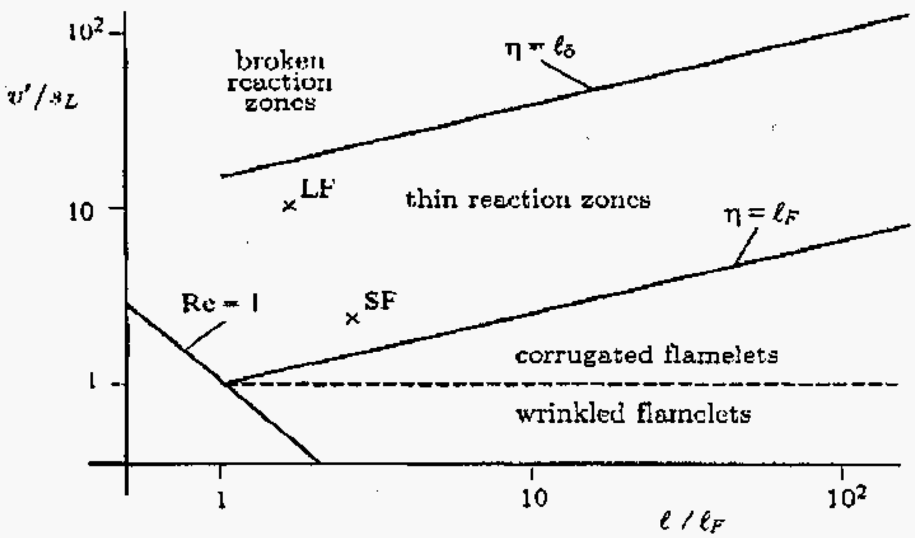

$10^2$
$v'/s_L$
10
1
broken reaction zones
$\eta = \ell_\delta$
LF
thin reaction zones
$\eta = \ell_F$
Re = 1
SF
corrugated flamelets
wrinkled flamelets
1
10
$10^2$
$\ell / \ell_F$


Figure 1:

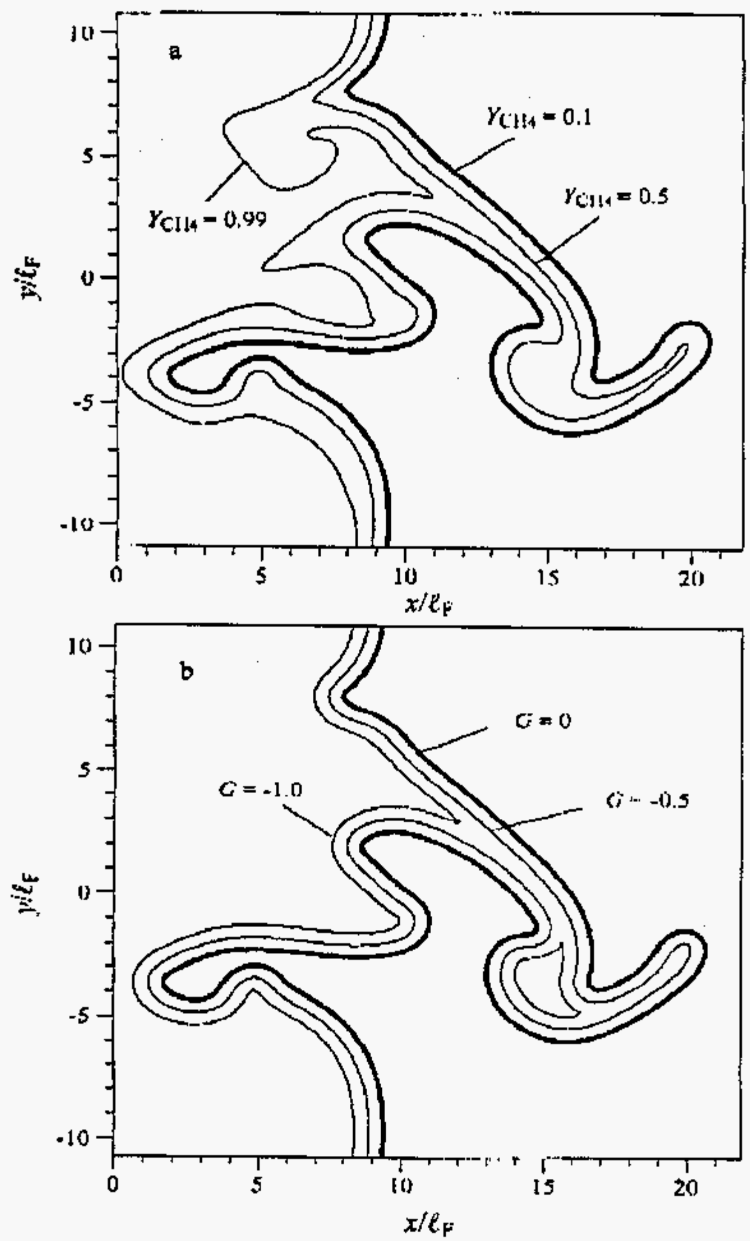


Figure 2:

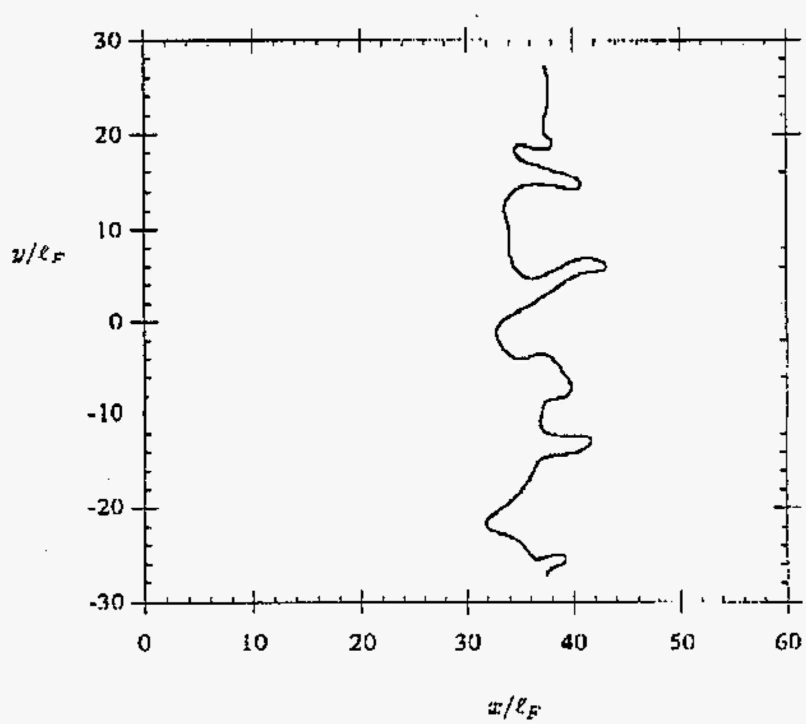


Figure 3:

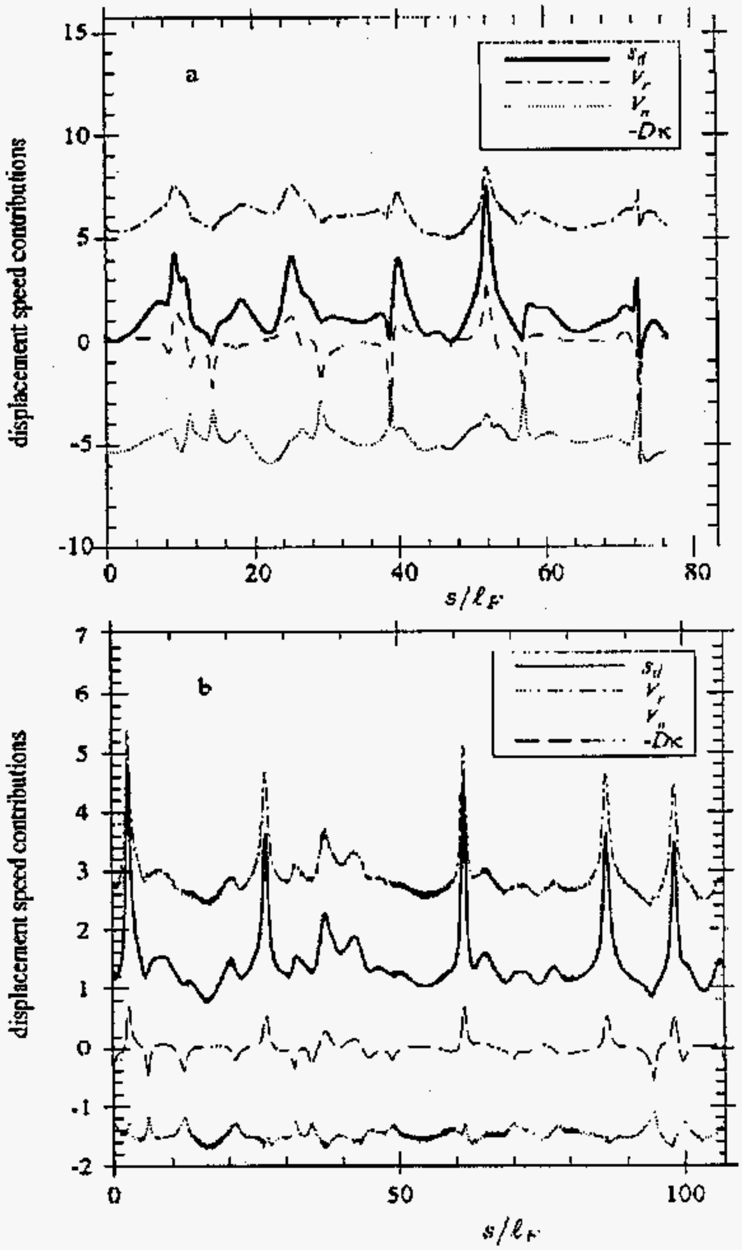

a
$s_d$
$V_r$
$V_n$
$-D\kappa$
displacement speed contributions
$s/\ell_F$
b
$s_d$
$V_r$
$V_n$
$-D\kappa$
displacement speed contributions
$s/\ell_F$


Figure 4:

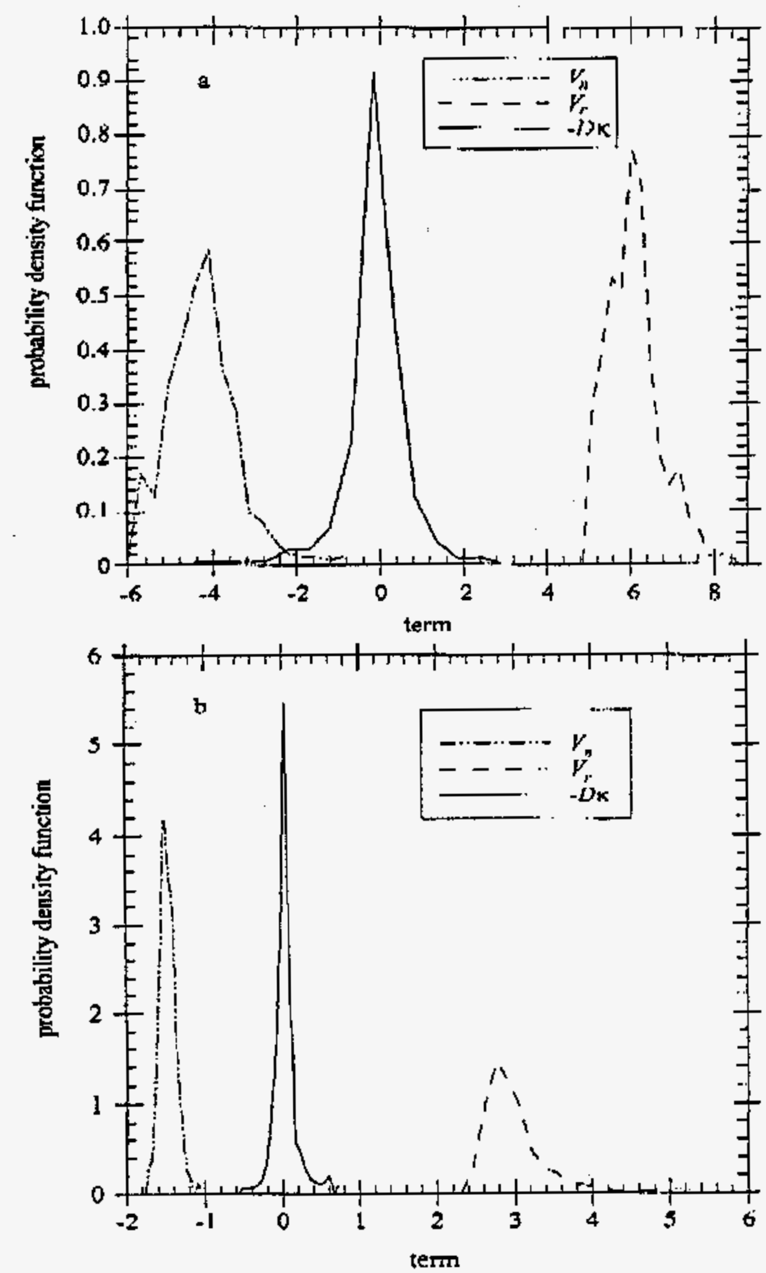

a
$V_n$
$V_r$
$-D\kappa$
probability density function
term
b
$V_n$
$V_r$
$-D\kappa$
probability density function
term


Figure 5:

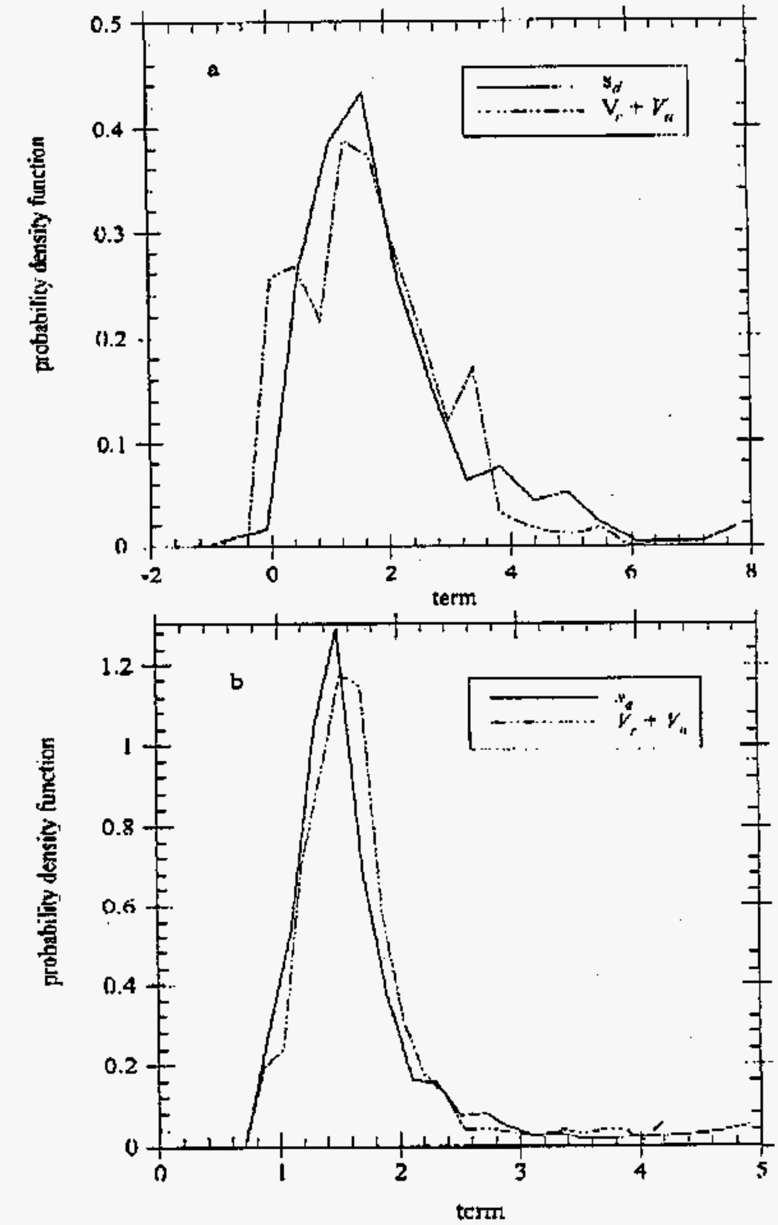
a
b
probability density function
term
0
0.1
0.2
0.3
0.4
0.5
-2
0
2
4
6
8
0.2
0.4
0.6
0.8
1
1.2
0
1
2
3
4
5

Figure 6:

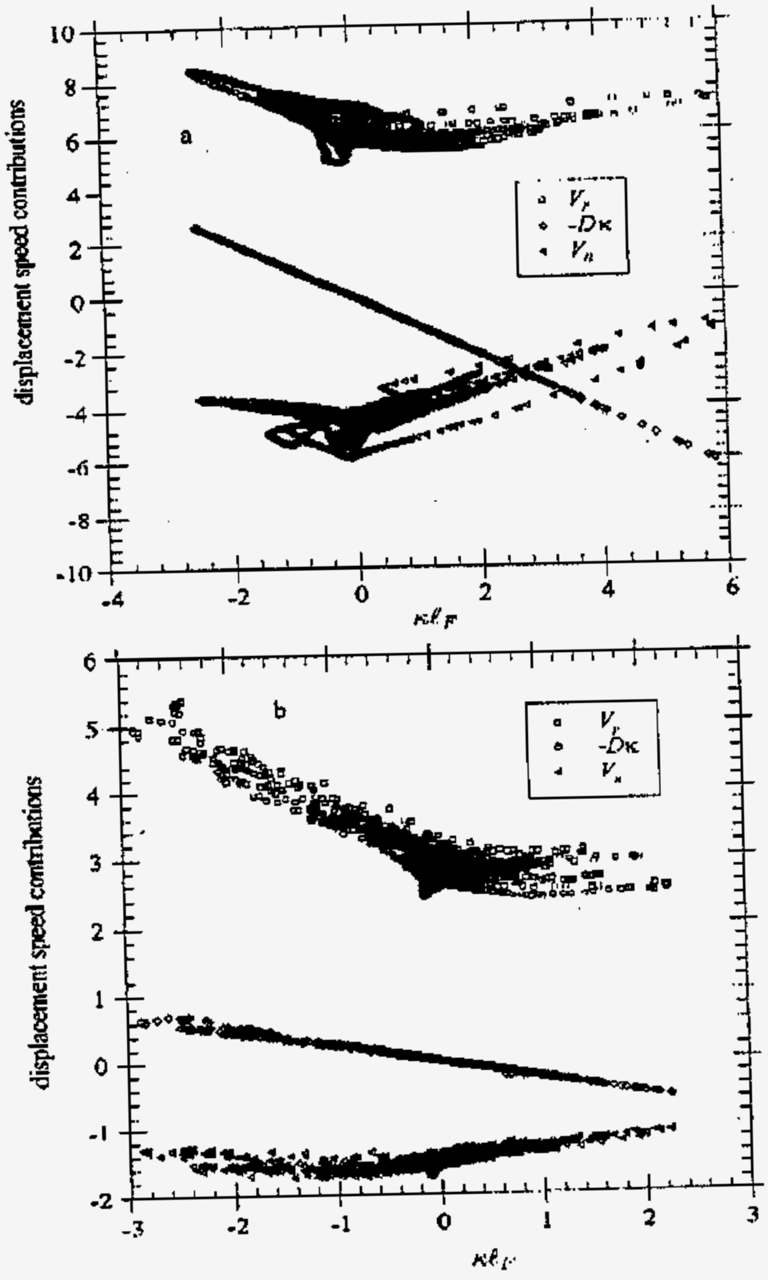

a
$V_F$
$-D\kappa$
$V_n$
displacement speed contributions
$\kappa \ell_F$
b
$V_F$
$-D\kappa$
$V_n$
displacement speed contributions
$\kappa \ell_F$


Figure 7:

## List of Figures

M98052539

Report Number (14) SAND--98-8481C
CONF-980804--

Publ. Date (11) 19971208
Sponsor Code (18) DOE/EE, XF
UC Category (19) UC-1409, DOE/ER





DOE